Chubb, C., & Sperling, G. (1989). Second-order motion perception: Space/time separable mechanisms. In *Proceedings: Workshop on Visual Motion (March 20-22, 1989, Irvine, California)* (pp. 126-138). Washington, DC: IEEE Computer Society Press.

Second-Order Motion Perception: Space/time Separable Mechanisms

Charles Chubb George Sperling

Human Information Processing Laboratory, Department of Psychology,
New York University, 6 Washington Place, New York, NY 10003

Abstract

Microbalanced stimuli are dynamic displays which do not stimulate motion mechanisms that apply *standard* (Fourier-energy or autocorrelational) *motion analysis* directly to the visual signal. Because they bypass such *first-order* mechanisms, microbalanced stimuli are uniquely useful for studying *second-order* motion perception (motion perception served by mechanisms that require a grossly nonlinear stimulus transformation prior to standard motion analysis). Some stimuli are *microbalanced under all pointwise stimulus transformations* and therefore are immune to early visual nonlinearities. We use them to disable motion information derived from spatial (temporal) filtering in order to isolate the temporal (spatial) properties of space/time separable second-order motion mechanisms. The motion of all of the microbalanced stimuli we consider can be extracted by (1a) band-selective spatial filtering and (1b) biphasic temporal filtering, nonzero in dc, followed by (2) a rectifying nonlinearity and (3) standard motion analysis.

1. Introduction.

Standard motion analysis. A visual display is described by $L(x,y,t)$, its luminance as a function of space, x,y, and time, t. We use the term *standard motion analysis* for any computation applied to L *that derives* L*'s motion from correlations of* L*-values across time and space.* Such computations are consonant with the *motion-from-Fourier-components principle*, which states that L's motion is reflected in some reasonable way by the contributions to L of individual Fourier components (drifting sinusoidal gratings). The recently proposed motion-perception theories of Adelson & Bergen [1], Heeger [5], van Santen & Sperling [3,4], and Watson & Ahumada [2] all perform various forms of standard motion analysis on their input. Similarly, the computer vision models of Anandan [9] and Waxman & Bergholm [10] also perform standard motion analysis on the input signal.

First-order mechanisms. A fundamental transformation generally presumed to be subjected to standard motion analysis in human visual processing is the *contrast* of the signal (the normalized deviation of luminance from its locally computed mean). We call mechanisms *first-order* that apply standard motion-analysis to raw stimulus contrast. Any motion mechanism that applies a grossly nonlinear transformation to the stimulus prior to standard motion analysis, we call *second-order*.

It is becoming clear, from apparently moving stimuli which do not stimulate standard motion detectors, that first-order mechanisms cannot account for all the data [11-28]. In particular, Chubb and Sperling [24,26,27] have demonstrated a variety of stimuli which display consistent, unambiguous apparent motion, yet which do not systematically stimulate first-order mechanisms.

The methods used by Chubb & Sperling [26] to construct apparent motion stimuli devoid of systematic first-order motion content are founded on the notion of a *microbalanced* random stimulus. A random stimulus I is *microbalanced* iff, for any space/time separable function W, the result $J = WI$ of multiplying I by W satisfies the following condition: (J is *drift balanced*) the expected power in J of any given drifting sinusoidal grating is equal to the expected power in J of the grating of the same spatial frequency, drifting at the same rate, but in the opposite direction. Drift-balanced and microbalanced random stimuli are useful for studying motion perception because they provide flexible access to *second-order* motion mechanisms without systematically engaging first-order mechanisms.

In this paper, we begin by reviewing the basic results about drift-balanced and microbalanced random stimuli, then apply these findings to generate a collection of microbalanced stimuli displaying various types of motion. The motion of each of the stimuli we consider is best revealed to standard analysis by a *space/time separable* linear filter followed by a rectifier. The first two microbalanced stimuli we discuss (stimuli 3.1 and 3.2) place important constraints on the *temporal* filtering mediating space/time separable, second-order motion-perception. The motion of each of the last four stimuli (4.2.2, 4.2.3, 4.2.5, and 4.2.6) depends only on the *spatial* filtering stage (temporal filtering alone, followed by rectification, cannot expose the motion of these stimuli).

A transformation is *pointwise* if its output value at a point (x,y,t) in space/time depends only on the value of the input at (x,y,t). Pointwise transformations include what are often called "static nonlinearities." Stimuli 3.2, 4.2.2, 4.2.3, 4.2.5 and 4.2.6 all *remain microbalanced after arbitrary pointwise transformations.* We present general methods for constructing stimuli of this sort.

CH2716-9/89/0000/0126$01.00 © 1989 IEEE

A transformation is *purely temporal* if its output value at a point (x, y, t) depends only on the history of input at (x, y). The class of purely temporal transformations is very general and includes, for example, temporal bandpass filtering preceded and followed by arbitrary pointwise transformations. Stimuli 4.2.2, 4.2.3, 4.2.5 and 4.2.6 *remain microbalanced after any purely temporal transformation.* Such stimuli are extremely useful for investigating second-order motion perception, because they provide a critical measure of control in differentially stimulating specific second-order mechanisms. Indeed, under virtually all models of visual processing, the first effective transformation mediating the perception of motion displayed by such stimuli is bound to be a *spatial linear filter* (a "texture-grabber"). This linear stage must, of course, be followed by a pointwise nonlinearity (such as rectification or thresholding) to expose the microbalanced stimulus motion to standard analysis.

2. Preliminaries.

Section outline. In this section we state the background facts presupposed by the main discussion of the paper. The broad topics covered are:

• **Real-valued, discrete visual stimuli and their Fourier transforms.** We take a stimulus to be a real-valued function whose action is restricted to a finite grid of spatiotemporal sampling locations.

• **Transformations.** Definitions are given of linear shift-invariant transformations, and pointwise transformations.

• **Random stimuli.** A random stimulus is a jointly distributed set of random variables assigned to a grid of spatiotemporal sampling locations.

• **Drift-balanced and microbalanced random stimuli.** A random stimulus I is drift balanced iff the expected power contributed to I by any given Fourier component (drifting-sinusoidal grating) is equal to the expected power in I of the grating of the same spatial frequency drifting at the same rate, but in the opposite direction. I is microbalanced iff WI is drift balanced for any space/time separable function W that "windows" I. The class of microbalanced random stimuli is significant for studying motion-perception, since (i) it is easy to construct a broad range of microbalanced random stimuli which display consistent, compelling apparent motion across independent realizations, despite the fact that (ii) the motion displayed by any microbalanced random stimulus is invisible to first-order mechanisms, regardless of the spatiotemporal scope over which they perform their motion-analysis.

uf with g by $f * g$, and the product of f with g by fg.

2.1. Discrete dynamic visual stimuli and their Fourier transforms.

We let $\mathbb{R}$ denote the real numbers, and $\mathbf{Z}$ ($\mathbf{Z}^+$) the integers (positive integers).

Contrast modulation. Luminance $l(x,y,t)$ is physically constrainted to be a non-negative quantity. Psychophysically, the significant quantity is *contrast*, the normalized deviation at each time t of luminance at each point (x,y) in the visual field from l_o a "background level", or "level of adaptation", which reflects the average luminance over points proximal to (x,y,t) in space and time. We shall restrict our attention throughout this paper to stimuli for which it can be assumed that the background luminance level l_o is uniform over the significant spatiotemporal locations in the display.

For any stimulus l with base luminance l_o, call the function I satisfying

$$l = l_o(1 + I),$$

the *contrast modulator* of l (and note that $I \geq -1$).

Psychophysically, it is well-established that over substantial ranges of l_o, the apparent motion of l does not depend upon l_o. Therefore, we shift our focus from luminance to contrast, and identify a stimulus with its contrast modulator, dropping reference to background level.

Stimuli. We restrict ourselves to discrete stimuli, whose activity is restricted to a finite grid of points in space/time. Specifically, we call any function $I:\mathbf{Z}^3 \to \mathbb{R}$ a *stimulus* iff $I[x,y,t] = 0$ for all but finitely many points of $\mathbf{Z}^3$. We shall be considering stimuli as functions of two spatial dimensions and time. The reader may find it convenient to think of the first spatial dimension (always indexed by x) as horizontal, with values increasing to the right, the second spatial dimension (indexed by y) as vertical, with values increasing upward. The temporal dimension is indexed by t. For concreteness, the reader is encouraged to imagine $\mathbf{Z}^3$ as indexing the pixels in a dynamic digital display.

Because any stimulus I is nonzero at only a finite number of points, the power in I is finite, from which we observe that I has a well-defined Fourier transform.

We denote I's Fourier transform by $\bar{I}$:

$$\bar{I}(\omega,\theta,\tau) = \sum_{x,y,t \in \mathbf{Z}} I[x,y,t]e^{-j(\omega x + \theta y + \tau t)}.$$

Although $\bar{I}$ is defined for all real numbers ω, θ, τ, it is periodic over 2π in each variable. This fact is reflected in the inverse transform:

$$I[x,y,t] = \frac{1}{(2\pi)^3}\int_0^{2\pi}\int_0^{2\pi}\int_0^{2\pi} \bar{I}(\omega,\theta,\tau)e^{j(\omega x + \theta y + \tau t)}\,d\omega\,d\theta\,d\tau.$$

In the Fourier domain, ω indexes frequencies relative to x, θ indexes frequencies relative to y, and τ indexes frequencies relative to t.

We distinguish the stimulus $\mathbf{0}$ by setting $\mathbf{0}[x,y,t] = 0$ for all $x,y,t \in \mathbf{Z}$.

Any stimulus I is called *space/time separable* if $I[x,y,t] = g[x,y]\,h[t]$, for some real-valued functions g and h of space and time respectively.

2.2. Transformations.

Any function T which takes the set of real-valued functions of $\mathbf{Z}^3$ into itself is called a *transformation*. If, for instance, $I:\mathbf{Z}^3 \rightarrow \mathbb{R}$ then $T(I):\mathbf{Z}^3 \rightarrow \mathbf{R}$, and we write $T(I)[x,y,t]$ to indicate the value of $T(I)$ at any point $(x,y,t) \in \mathbf{Z}^3$. We shall be particularly concerned with two types of transformations: *linear shift-invariant* transformations, and *pointwise* transformations.

Pointwise transformations, rectifiers. For any functions $f: A \rightarrow B$ and $g: B \rightarrow C$, the *composition* $g \bullet f: A \rightarrow C$ is given by

$$g \bullet f(a) = g(f(a))$$

for any $a \in A$. Then for any $f:\mathbf{R} \rightarrow \mathbf{R}$, we call the transformation $f\bullet$, yielding the spatiotemporal function $f \bullet I$ when applied to stimulus I, a *pointwise* transformation (because its output value at any point in space/time depends only on its input value at that point). The transformation $f\bullet$ is called a *positive half-wave rectifier* if f is monotonically increasing, and $f[v] = 0$ for all $v \leq 0$. $f\bullet$ is called a *negative half-wave rectifier* if f is monotonically decreasing, and $f[v] = 0$ for $v \geq 0$. Finally, $f\bullet$ is called a *full-wave* rectifier if f is a monotonically increasing function of absolute value.

Linear, shift-invariant transformations. Linear, shift-invariant (LSI) transformations are spatiotemporal convolutions: For $k:\mathbf{Z}^3 \rightarrow \mathbf{R}$ (the *impulse response*), the LSI transformation $k*$ yields the convolution $k * I$ when applied to any stimulus I: i.e., for any $\alpha \in \mathbf{Z}^3$,

$$k * I[\alpha] = \sum_{\beta \in \mathbf{Z}^3} I[\beta]\, k[\alpha - \beta].$$

2.3. Random stimuli.

The notion of a random stimulus generalizes that of a nonrandom stimulus in that the values assigned points in space/time by a random stimulus are random variables rather than constants. A random stimulus is a family $\{R[x,y,t] \mid x,y,t \in \mathbf{Z}\}$ of random variables, all but some finite number of which are always 0. To ensure that R has a well-defined expected power spectrum we require that $R[x,y,t]$ has a finite second moment for each $(x,y,t) \in \mathbf{Z}^3$:

2.3.1. Call any family $\{R[x,y,t] \mid (x,y,t) \in \mathbf{Z}^3\}$ of jointly distributed random variables a *random stimulus* provided

(i) for all but finitely many $(x,y,t) \in \mathbf{Z}^3$, $R[x,y,t]$ is invariably equal to 0,

and

(ii) $E\left[R[x,y,t]^2\right]$ exists for all $(x,y,t) \in \mathbf{Z}^3$.

As with non-random stimuli, we write $\bar{R}$ for the Fourier transform of the random stimulus R. R is called *space/time* separable iff R is space/time separable with probability 1. If there exists a stimulus S such that $R = S$ with probability 1, then R is called *constant*.

2.4. Drift-balanced and microbalanced random stimuli.

The *motion-from-Fourier-components principle* is a commonly encountered rule of thumb for predicting the apparent motion of an arbitrary stimulus $I[x,y,t] = f[x,t]$ that is constant in the vertical dimension of space. It states that, for I considered as a linear combination of drifting sinusoidal gratings, if the power in I of the rightward-drifting gratings is greater than the power of the leftward-drifting gratings, then apparent motion should be to the right. Conversely, if most of I's power resides in the leftward-drifting gratings, apparent motion should be to the left. Otherwise I should manifest no decisive motion in either direction.

This prediction rule for horizontally moving stimuli is a restricted version of the more general *motion-from-Fourier-components* principle: For any stimulus L to exhibit motion in a certain direction in the neighborhood of some point $(x,y,t) \in \mathbf{Z}^3$, there must be some spatiotemporal volume Δ proximal to (x,y,t) such that the Fourier transform of L computed locally across Δ has substantial power over some regions of the frequency domain whose points correspond, in the space/time domain, to sinusoidal gratings drifting in a direction consistent with the motion perceived.

The following class of random stimuli provides a rich pool of counterexamples to the motion-from-Fourier-components principle [26].

2.4.1. Call any random stimulus R *drift balanced* iff

$$E\left[|\bar{R}(\omega,\theta,\tau)|^2\right] = E\left[|\bar{R}(\omega,\theta,-\tau)|^2\right]$$

for all $(\omega,\theta,\tau) \in \mathbf{R}^3$.

Thus, a random stimulus R is drift balanced iff the expected power in R of each drifting sinusoidal component is equal to the expected power of the component of the same spatial frequency, drifting at the same rate, but in the opposite direction. That is, that expected power of every frequency is the same, independently of whether a series of frames is displayed in forward or reverse order. Obviously, for any class of spatiotemporal receptors tuned to stimulus power in a certain spatiotemporal frequency band, a drift-balanced random stimulus will, on the average, stimulate equally well those receptors tuned to the corresponding band, of opposite temporal orientation.

Microbalanced Random Stimuli. Consider the following two-flash stimulus S: In flash 1, a bright spot (call it Spot 1). appears. In flash 2, Spot 1 disappears, and two new spots appear, one to the left and one symmetrically to the right of Spot 1. As one might suppose, S is drift balanced. On the other hand, it is equally clear that a first-order motion detector whose spatial reach encompassed the location of Spot 1 and only *one* of the Spots in flash 2 might well be stimulated in a fixed direction by S. Thus, although S is drift balanced, some first-order motion-detectors may be stimulated strongly and systematically by S. These detectors can be differentially selected by *spatial windowing*, and thereby the drift-balanced stimulus S can be converted into a non-drift-balanced stimulus by multiplying it by an appropriate space/time separable

function. This property is escaped by the following subclass of drift-balanced random stimuli.

2.4.2. Call any random stimulus I *microbalanced* iff WI is drift balanced for any space/time separable (non-random) function W.

One can think of the multiplying function W as a "window" through which a spatiotemporal subregion of I can be "viewed" in isolation. The space/time separability of W insures that it is "transparent" with respect to the motion-content of the region of to which it is applied: W does not distort I's motion with any motion content of its own. Thus, the fact that I is microbalanced means that any subregion of I encountered through a "motion-transparent window" is drift balanced.

The following characterization of the class of microbalanced random stimuli, and the rest of the results in this section are from Chubb and Sperling [26].

2.4.3. *A random stimulus I is microbalanced if and only if*

$$E\Big[I[x,y,t]\,I[x',y',t'] - I[x,y,t']\,I[x',y',t]\Big] = 0$$

for all $(x,y,t),(x',y',t') \in \mathbf{Z}^3$.

Some other relevant facts about microbalanced random stimuli:

2.4.4. *For any independent microbalanced random stimuli I and J,*

I. *the product IJ is microbalanced,*

and

II. *the convolution $I * J$ is microbalanced.*

2.4.5. *(a) Any space/time separable random stimulus is microbalanced; (b) any constant microbalanced random stimulus is space/time separable.*

The following result is useful in constructing a wide range of microbalanced random stimuli which display striking apparent motion.

2.4.6. *Let Γ be a family of pairwise independent, microbalanced random stimuli, all but at most one of which have expectation $\mathbf{0}$. Then any linear combination of Γ is microbalanced.*

The Reichardt detector characterization of microbalanced random stimuli. Two first-order motion detectors proposed for psychophysical data [1,6] can be recast as variants of a *Reichardt Detector* [3,4,31]. The Reichardt detector has many useful properties as a motion detector without regard to its specific instantiation [3,4].

Figure 1 shows a diagram of the Reichardt detector. The Reichardt detector consists of a left and a right subunit that share their inputs. The left subunit normally computes leftward motion because the filter g_1* acts as an internal delay to match the external delay of a moving stimulus. The right subunit normally computes rightward motion. The output represents the smoothed leftward minus rightward difference.

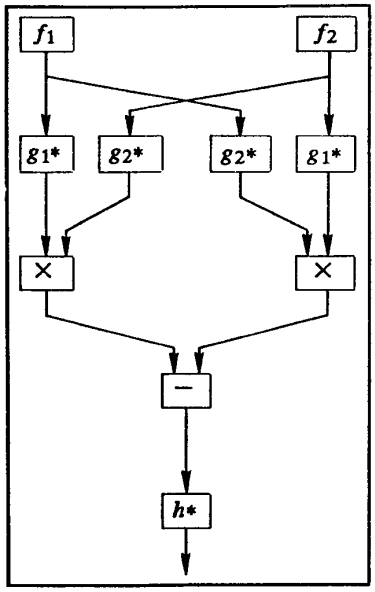

Figure 1: *The Reichardt detector.* The detector consists of a left and a right subunit; the left unit normally detects leftward movement; the right unit, rightward movement. In response to a stimulus I, each spatial input filter (receptive field) f_i outputs a temporal function that is then convolved with a temporal filter g_i*. The correlator boxes, marked "×", ouput the product of their inputs. The box marked "−" outputs its left input minus its right; this output indicates the net leftward minus rightward motion. The box $h*$ contains a temporal smoothing filter to produce time-averaged output.

Specifically, the Reichardt detector consists of spatial receptors characterized by spatial window functions (receptive fields) f_1 and f_2, temporal filters g_1* and g_2*, multipliers, a differencer, and another temporal filter $h*$. The spatial receptors f_i, $i = 1, 2$, act on the input stimulus I to produce intermediate outputs,

$$y_i[t] = \sum_{(x,y)\in\mathbf{Z}^2} f_i[x,y]\,I[x,y,t].$$

At the next stage, each temporal filter g_j* transforms its input y_i $(i, j = 1, 2)$, yielding four temporal output functions: $g_j * y_i$. The left and right multipliers then compute the products

$$\Big[y_1 * g_1[t]\Big]\Big[y_2 * g_2[t]\Big] \quad \text{and} \quad \Big[y_1 * g_2[t]\Big]\Big[y_2 * g_1[t]\Big]$$

respectively, and the differencer subtracts the output from the right multiplier from that of the left multiplier:

$$D[t] = \Big[y_1 * g_1[t]\Big]\Big[y_2 * g_2[t]\Big] - \Big[y_1 * g_2[t]\Big]\Big[y_2 * g_1[t]\Big].$$

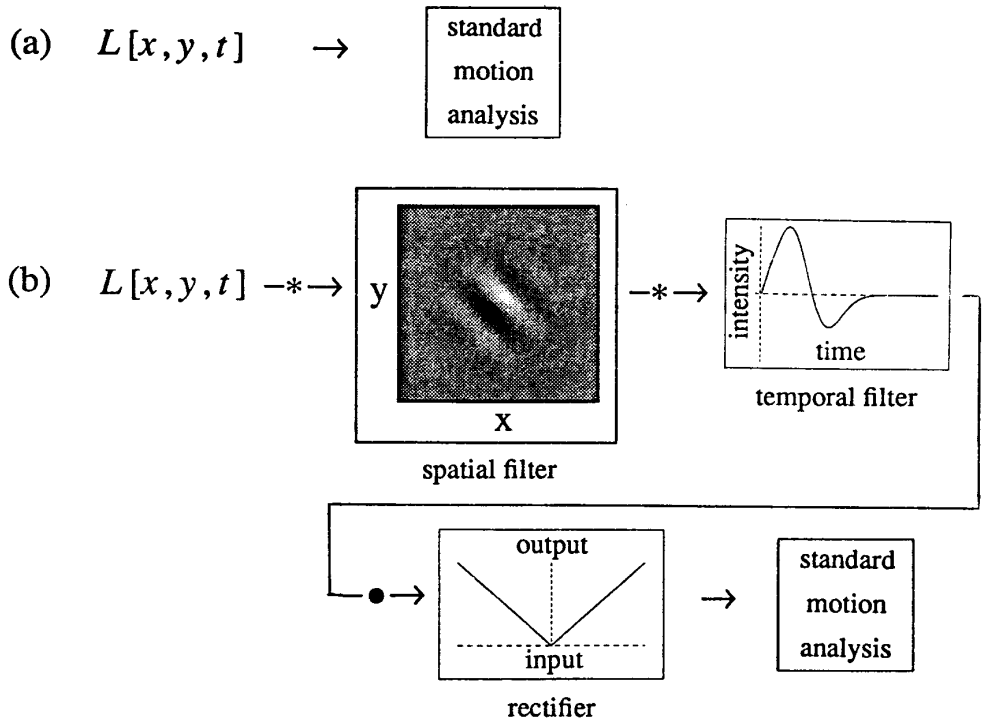

Figure 2: *First-order and second-order motion mechanisms.* (a) First-order motion mechanisms apply standard motion analysis (e.g., Reichardt model) directly to the luminance signal L. Many second-order mechanisms can be modeled by a signal transformation comprised of a spatiotemporal linear filter followed by a pointwise nonlinearity followed by standard motion analysis. The filtering performed in (b) is *space/time separable* (spatial filtering and temporal filtering occur in separate boxes), followed by a pointwise nonlinearity, which is illustrated here with a full-wave rectifier. The motion of all the microbalanced stimuli considered in this paper can be extracted by the second-order mechanisms diagrammed in (b) with appropriately chosen spatial and temporal filters.

The final output is produced by applying the filter $h*$, whose purpose is to appropriately smooth the time-varying, differencer output D. Since almost all first-order mechanisms can be expressed as, or closely approximated by Reichardt detectors, the following result [27] is the cornerstone of the claim that microbalanced random stimuli bypass first-order motion mechanisms.

2.4.7. *For any random stimulus I, the following conditions are equivalent:*

(a) I is microbalanced.

(b) The expected response of any Reichardt detector to I is 0 at every instant in time.

Varieties of microbalanced motion.

In Sections 3 and 4, we describe six random stimuli, all of which are microbalanced, yet display consistent apparent motion across independent realizations. For each of these random stimuli I, the motion displayed by I can be exposed to standard motion analysis by a transformation

$$T(I) = r \bullet (f * I) \ , \qquad (1)$$

where $r \bullet$ is a rectifier, and $f*$ is a space/time separable filter.

3. Motion mediated by simple rectification and by temporal differentiation followed by rectification.

The first two stimuli (3.1 and 3.2) place constraints only on the temporal component of the the filter $f*$. Subsequent stimuli focus on the spatial component.

3.1. Stimulus: The amplitude-modulating squarewave. The motion of some of the microbalanced stimuli demonstrated by Chubb & Sperling [24,26] results from modulating the *amplitude* of spatially independent, visual noise. For example, Fig. 3a shows an xt cross-section of a squarewave, stepping 1/4 spatial-cycle leftward each frame, modulating (between 0 and 1) the amplitude of a row of static, horizontally independent black/white vertical bars. This stimulus displays obvious leftward motion to all viewers under a broad range of viewing

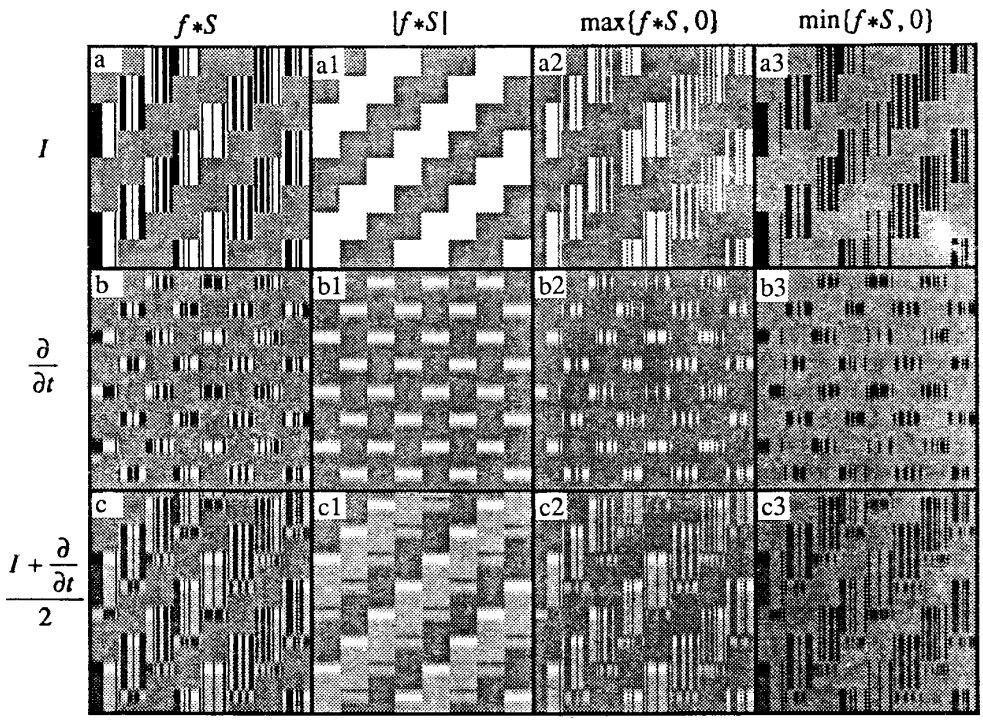

Figure 3: *Transformations of the contrast-modulating squarewave.* All 12 panels are *xt* cross-sections (with time running downward) of various transformations of stimulus 3.1, the *contrast-modulating squarewave*. Stimulus 3.1 itself is cross-sectioned in (a). The horizontal dimension is x, the vertical dimension is t with time increasing downward, and the stimulus is unvarying in y. The problem of perceiving leftward motion in the dynamic display whose *xt* cross section is represented by panel (a) is equivalent to the texture problem of perceiving orientation slanting down and to the left in the panel (a) itself. In the left-hand column are displayed cross-sections of 3 linear transformations of the stimulus: (a) the identity, (b) the partial derivative with respect to time, and (c) the average of the operators applied in (a) and (b). The next column (a1, b1, c1) shows the result of full-wave rectification (absolute value) of the corresponding (same-row) linear transformations; e.g., (a1) shows the result of full-wave rectifying the untransformed stimulus 3.1. Column three shows the positive half-wave components of the same-row linear transformations in column 1; column 4 shows the negative half-wave components. The functions in column 1 (linear transformations of the contrast-modulating squarewave) are all microbalanced; hence, the right-to-left motion displayed by the stimulus cannot be obtained from these transformations by standard motion analysis. Temporal differentiation (the second-row transformations) yields motion-ambiguous functions; rows 1 and 3 yield functions whose motion is extractable by standard motion analysis.

conditions, despite the fact that (as is easily proven from propositions 2.4.5a and 2.4.6) it is microbalanced.

Simple rectification exposes the motion of the amplitude-modulating squarewave. As suggested by Figs. 3a1, 3a2, and 3a3, simple full-wave or half-wave rectification (i.e. setting $f*$ to the identity in Eq. (1)) suffices to expose motion carried by amplitude-modulation. However, simple rectification fails to expose the motion in the following stimulus.

3.2. Stimulus: The contrast-reversing squarewave. A sideways stepping squarewave is used to alternately multiply the *contrast* of spatially independent noise by +1 and −1. Fig. 4a shows an *xt* cross-section of a squarewave that steps leftward 1/4 spatial-cycle at regular temporal intervals, reversing the *contrast* of black/white vertical bars as it moves. Like the amplitude-modulating squarewave, this contrast-reversing squarewave displays vivid leftward motion to all viewers under a broad range of viewing conditions; nonetheless, it is microbalanced (another easy consequence of propositions 2.4.5a and 2.4.6).

Simple rectification fails to reveal the motion of the contrast-reversing squarewave. As illustrated in Figs. 4a1, 4a2 and 4a3, simple rectification does not expose the motion of the contrast-reversing squarewave to standard motion analysis: full-wave rectification yields a uniform field, while half-wave rectification yields a mere dc-shifted rescaling of the original stimulus. Indeed, any purely spatial filter followed by rectification is equally ineffective at revealing this motion [27].

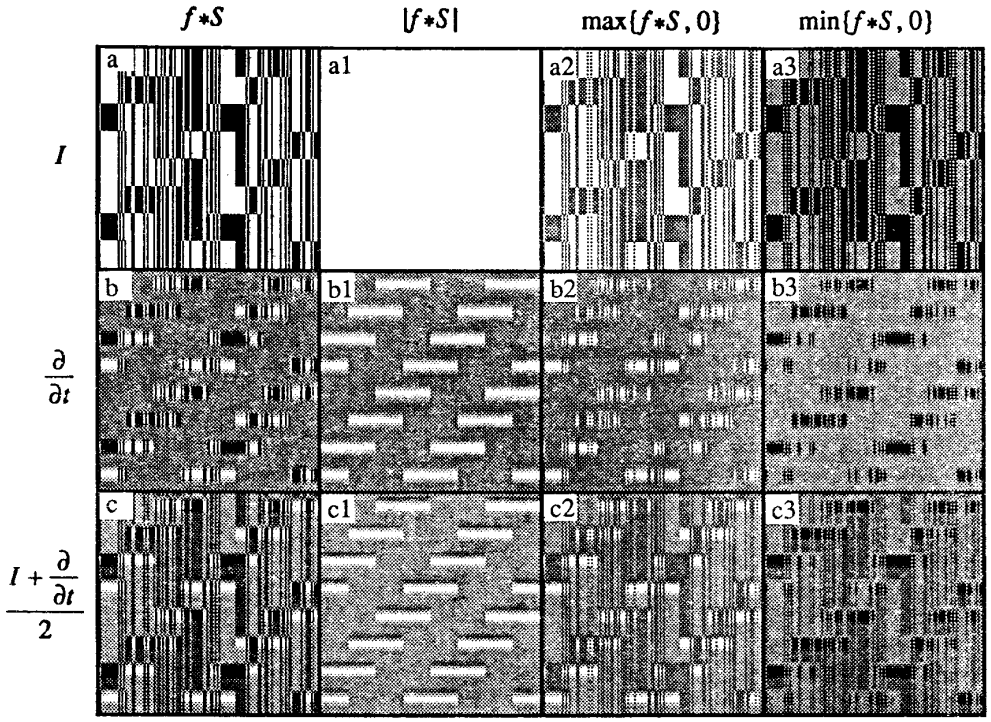

Figure 4: *Transformations of the contrast-reversing squarewave.* All 12 panels are *xt* cross-sections (with time running downward) of various transformations of stimulus 3.2, the *contrast-reversing squarewave*, which is itself is cross-sectioned in (a). See caption of Fig. 3 for a description of the transformations and panel arrangement. All of the functions in the left column (the linear transformations of the contrast-reversing squarewave) are microbalanced, so the right-to-left motion displayed by the stimulus cannot be obtained from these transformations by standard motion analysis. The purely pointwise transformations (the rectifications shown in the first row) also yield microbalanced functions and hence no simply-accessible motion. However, after any of the rectifying transformations in rows (b) or (c), the stimulus motion is accessible to standard motion analysis.

Temporal differentiation followed by rectification reveals the motion of the contrast-reversing squarewave. The obvious transformation to expose the motion of this stimulus to standard motion analysis is *temporal differentiation* followed by half-wave or full-wave *rectification*. The result of differentiating the contrast-reversing squarewave with respect to time is shown in Fig. 4b. The motion of this temporal derivative remains microbalanced (a consequence of propositions 2.4.4 II. and 2.4.5a). However, as suggested by Figs. 4b1, 4b2 and 4b3, either full-wave (Fig. 4b1) or half-wave (Figs. 4b2 & 4b3) rectification suffices to reveal the motion of the temporal derivative of the contrast-reversing squarewave to standard analysis. However,

Temporal differentiation followed by rectification fails to expose the motion of the amplitude-modulating squarewave. Differentiating the *amplitude-modulating* squarewave (Fig. 3a) with respect to time *sacrifices* all the motion content of this stimulus (See. Fig. 3b). The differentiated stimulus (Fig. 3b) is completely ambiguous in motion-content, and subsequent transformations (e.g. full- or half-wave rectification: Figs. 3b1, 3b2, 3b3) cannot reclaim the original stimulus motion.

To recapitulate: The motion of the amplitude-modulating squarewave (Fig. 3a) is exposed by simple half-wave or full-wave rectification (Figs. 3a1, 3a2, 3a3). However, rectification fails to expose the motion of the contrast-reversing squarewave (signal in Fig. 4a; rectifications in Figs. 4a1, 4a2, 4a3). On the other hand, temporal differentiation followed by half-wave or full-wave rectification suffices to expose the motion of the contrast-reversing squarewave to standard analysis (Figs. 4b, 4b1, 4b2, 4b3), but fails to reveal the motion of the amplitude-modulating squarewave (Figs. 3b, 3b1, 3b2, 3b3).

A single transformation which reveals the motion of both stimuli 3.1 and 3.2 to standard motion-analysis can easily be obtained by letting $f*$ of Eq. (1) be a temporal linear filter (spatial component = identity) with impulse response given by Fig. 5.

The result of applying such a filter to the contrast-modulating squarewave is shown in Fig. 3c. As Figs. 3c1, 3c2, and 3c3 suggest, full- or half-wave rectification of the output (Fig. 3c) exposes the motion of the contrast-modulating square to standard analysis. And as Figs. 4c, 4c1, 4c2 and 4c3 indicate, the same transformations expose the motion of the contrast-reversing squarewave to standard analysis.

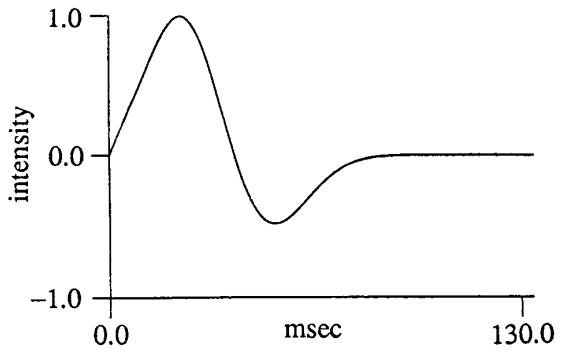

Figure 5: The impulse response of a temporal filter suitable to extract the motion of the contrast-modulating squarewave (Fig. 3a), and of the contrast-reversing squarewave (Fig. 4a). The filtered responses are shown in Figs. 3c and 4c. Subsequent rectification makes the motion accessible to standard motion analysis (see bottom row of Figs. 3 and 4).

4. Motion carried purely by spatial texture.

There are many microbalanced random stimuli whose motion depends on the spatiotemporal modulation of *spatial texture*. The most obvious transformations to expose texturally conveyed motion to standard motion analysis are given by $T(I) = r \bullet (f * I)$, with the separable filter $f*$ being purely spatial (temporal component = identity). The spatial filter $f*$ should be viewed as a "texture-grabber". $f*$ will respond with varying power throughout regions of the visual field, depending on whether or not the texture to which it is tuned populates those regions. However, the output of a linear filter to a texture is positive or negative according to the phase of the texture. That is, multiplying the contrast of the texture by -1 will multiply the filter's output by -1. The purpose of rectification is to report the presence or absence of texture, independent of phase. The result $T(I)$ is a spatiotemporal function whose value reflects the movement of the $(f*)$–texture across the visual field as a function of time. Elaborations of this scheme have been applied to modeling texture perception by Caelli [32], Bergen & Adelson [33], and Sutter, Beck & Graham [34].

To study texturally conveyed motion, it is important to bypass not only first-order motion mechanisms, but also irrelevant second-order mechanisms, such as the temporal mechanisms proposed above for accessing the motion of the amplitude- and contrast-reversing squarewaves—stimuli 3.1 and 3.2). A particular subclass of microbalanced random stimuli serves this purpose.

4.1. Random stimuli microbalanced under all pointwise transformations.

Many signal transformations encountered in perceptual models can be expressed as cascades of pointwise $(r\bullet)$ and space/time separable LSI transformations $(f*)$. For visual processing that is limited to such cascades, the following question is of considerable interest: What conditions must be satisfied by a random stimulus I in order that $r \bullet I$ be microbalanced for any function $r:\mathbb{R} \rightarrow \mathbb{R}$? For any such I, the cascade $f*(r\bullet I)$ does not suffice to reveal I's motion to standard analysis, as each successive transformation leaves the stimulus microbalanced. Thus I's motion can only be perceived by a mechanism which applies a cascade that includes a nontrivial LSI transformation followed by a pointwise nonlinearity.

Indeed, we have already encountered a simple example of such a stimulus, the contrast-reversing squarewave, stimulus 3.2, which we shall call J in this discussion. We demonstrated above that simple rectification cannot expose the motion of J to standard analysis, and it is easy to see that this observation generalizes beyond rectifiers to all pointwise transformations: Any pointwise transformation applied to J yields a rescaled version of J plus a constant. Input and output are both microbalanced.

The motion carried by the contrast-reversing squarewave J is exposed by rectifying the output of certain LSI transformations (e.g. the temporal derivative) of J. However, no pointwise transformation applied by itself to J suffices to expose J's motion content to standard analysis. In studying the processing stages that mediate second-order motion perception, it may be of some importance to know that a given stimulus is "immune" to a certain transformation or a certain type of transformation (as J is immune to pointwise transformations). This motivates the following notion [27]:

4.1.1. Call any random stimulus I microbalanced *under* a given transformation T iff $T(I)$ is microbalanced.

In connection with pointwise transformations, we have the following two results [27]:

4.1.2. *Let I be a random stimulus such that, for any $(x,y,t),(x',y',t') \in \mathbf{Z}^3$, $I[x,y,t]$ and $I[x',y',t']$ have a continuous joint density. Then the following conditions are equivalent:*

1. I is microbalanced under all pointwise transformations.

2. The joint density f of $I[x,y,t]$ with $I[x',y',t']$ and the joint density g of $I[x,y,t']$ with $I[x',y',t]$ satisfy

$$f(p,q) + f(q,p) = g(p,q) + g(q,p)$$

for all $p, q \in \mathbf{R}$.

4.1.3. (Corollary) *For any random stimulus I, if the joint density of $I[x,y,t]$ with $I[x',y',t']$ is identical either to the joint density of $I[x,y,t']$ with $I[x',y',t]$ or to the joint density of $I[x',y',t]$ with $I[x,y,t']$ for every $(x,y,t),(x',y',t') \in \mathbf{Z}$, then I is microbalanced under all pointwise transformations.*

4.2. Texture quilts.

The results of section 4.1 can easily be applied to construct a wide variety of stimuli for which the first effective stage of processing for motion involves a non-pointwise

transformation. If, as most models presume, processing channels are restricted to cascaded pointwise and LSI transformations, then this initial transformation must be (non-trivially) LSI. By themselves, however, LSI operators are insufficient to expose the motion of microbalanced random stimuli to standard analysis.

Thus, interposed between the initial LSI transformation and standard motion analysis there must be a (nonlinear) pointwise transformation. For the contrast-reversing squarewave, the LSI transformation of temporal differentiation followed by the pointwise transformation of full-wave rectification suffices to expose the motion to standard analysis.

Like the contrast-reversing squarewave, the following stimuli (i) are microbalanced under all pointwise transformations, and (ii) display consistent apparent motion across independent realizations. Unlike the contrast-reversing squarewave, the texture-grabbing filters appropriate for the following stimuli are spatial rather than temporal. In fact, it can be shown [27] that each of the stimuli I presented in this section is microbalanced *under all purely temporal transformations*; i.e., under all transformations whose output at a given point (x, y, t) in space/time depends only on the history of input at the spatial point (x, y). Thus, none of the transformations that sufficed to expose the motion of the amplitude-modulating and contrast-reversing squarewaves would reveal the motion of I to standard motion analysis.

All the examples of this section exploit the same essential trick: briefly displayed patches of static, random-phased texture occur in specific spatiotemporal relations to each other, and appropriate measures are taken to ensure that the resulting stimulus is microbalanced under all pointwise transformations. We call such stimuli *texture quilts*. The texture quilts constructed in our examples (exemplars are shown in Figs. 6b, 7d, 8b and 8c) all display decisive apparent motion from left to right, when viewed either monocularly or binocularly from a distance such that they span about 4 horizontal retinal degrees, with frames displayed at 15 Hz.

Binary texture quilts.

The easiest constructions of quilts that are microbalanced under all purely temporal transformations use stimuli that have only two contrast values. We show how to construct a generic binary-valued quilt and provide some specific examples.

4.2.1. A general technique for constructing binary texture quilts that are microbalanced under all purely temporal transformations. Let $\alpha \subset \mathbf{Z}^2$ be a set of points in space (those which will take nonzero values at some time during the display). For the number N of frames comprising the quilt, associate with frames 1 through N a family

$$\phi_1, \phi_2, \ldots, \phi_N$$

of jointly independent random variables, each of which takes the value 1 or -1 with equal probability. In addition, associate with frames 1 through N, a family

$$f_i, \quad i = 1, 2, \ldots, N$$

of functions, with f_i assigning 0 throughout all frames except the i^{th}, and within frame i, assigning 0 everywhere except α, with α being mapped into $\{1, -1\}$. Then, construct the stimulus

$$B = \phi_1 f_1 + \phi_2 f_2 + \ldots + \phi_N f_N.$$

It is easily derived from corollary 4.1.3 that B is microbalanced under all pointwise transformations. The proof that B is microbalanced under all purely temporal transformations is in [27].

4.2.2. Stimulus: The sidestepping, randomly contrast-reversing, vertical edge. Figure 6b displays nine frames comprising a particularly simple binary texture quilt. Note that the vertical dimension of Fig. 6b combines time and vertical space. The representation in Fig. 6b is precisely equivalent to a strip of movie film with frames arranged vertically above each other, separated by grey lines. Between successive grey lines is displayed the actual two-dimensional luminance function displayed to subjects. Fig. 6a shows the functions f_1 through f_9 used in the construction. f_1 assigns the value -1 to all points (x, y, t) within the spatiotemporal block of the first frame, and 0 to all other points. f_2 assigns the value 1 to the points in the leftmost eighth of the second frame, the value -1 to the points in the right seven eighths, and 0 to all points outside the second frame. The functions coloring successive frames shift the bright/dark edge rightward through the frame until in frame 9, the field is uniformly bright. Multiplying each frame $i = 1, 2, \ldots, 9$ by its associated random variable ϕ_i yields, in this particular realization, the stimulus given in Fig. 6b.

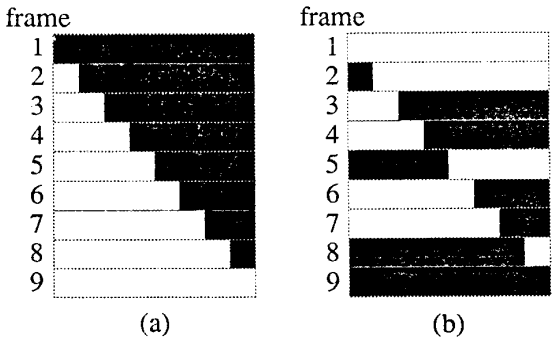

Figure 6: *Edge-driven motion from an ordinary edge and from a binary texture quilt.* (a) A rightward moving light/dark edge visible to first- and second-order motion detectors. Nine frames are shown; each frame shows exactly what is displayed, an area of contrast +1 and area of contrast −1. (b) A realization of the *sidestepping, randomly contrast-reversing vertical edge.* This random stimulus is microbalanced under all purely temporal transformations; therefore its rightward motion remains inaccessible to standard motion analysis even after an arbitrary, purely temporal transformation. Each of the frames 1 – 9 of (b) was derived from the corresponding frame of (a) by multiplying that entire frame by a random variable that takes the value 1 or −1 with equal probability. The nine frame random variables are jointly independent.

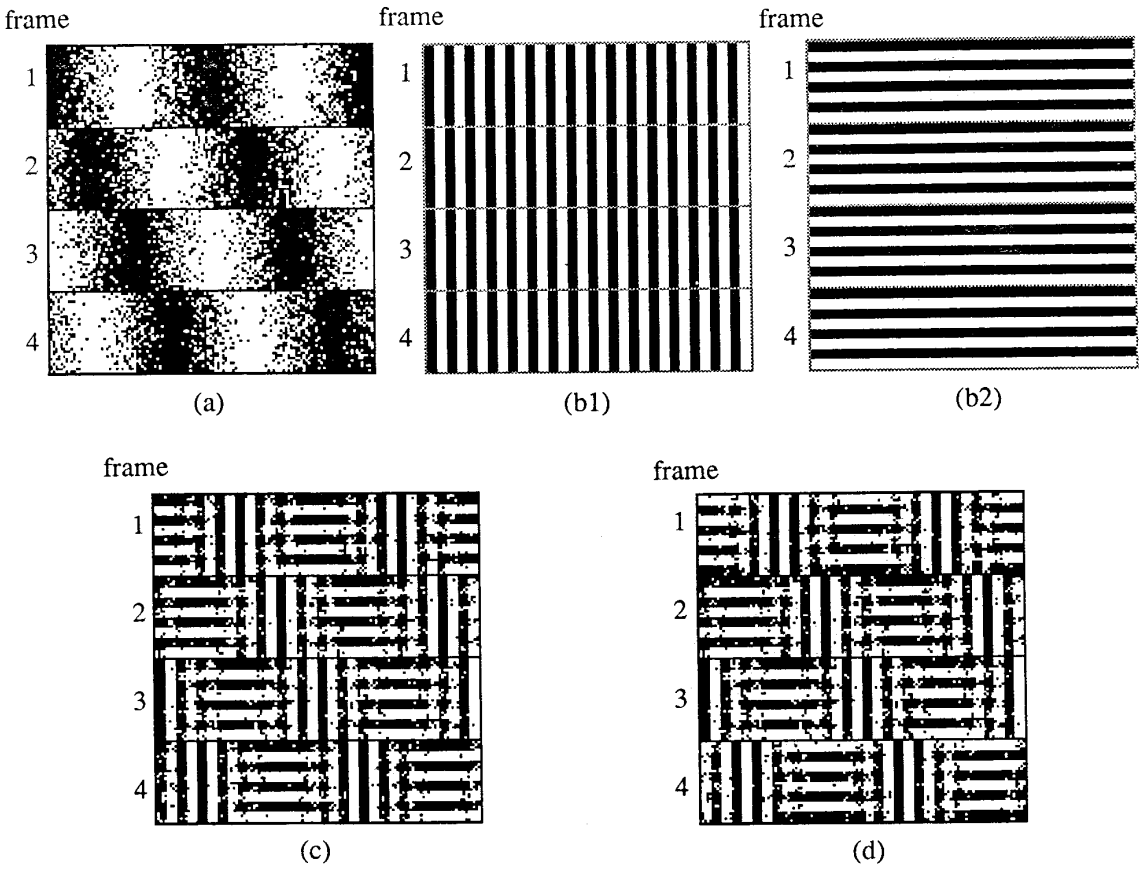

Figure 7: *Orientation-driven second-order motion from a binary texture quilt.* (a) Four frames of a probabilistically defined sinewave grating that steps rightward 90 degrees between frames. The rightward motion in (a) is accessible to all motion detectors. (b1) Four frames of a static, vertical squarewave grating; (b2) Four frames of a static horizontal squarewave grating. (c) A rightward translating texture pattern. For every white point in (a), the corresponding value in (c) is chosen from the vertical square-wave grating in (b1); for every black point, the corresponding value in (c) is chosen from the horizontal square-wave grating in (b2). Stimulus (c) is not microbalanced; its motion is accessible to standard motion analysis. (d) A texture quilt. The frames of (d) are derived by multiplying the corresponding frames of (c) by jointly independent random variables, each of which takes the value 1 or -1 with equal probability. The texture quilt realized in (c) is microbalanced under all purely temporal transformations; therefore its rightward motion is unavailable to standard motion analysis, even after an arbitrary, purely temporal transformation.

The motion displayed by this quilt is clearly driven by the randomly contrast-reversing edge that steps from left to right through the course of the display. Almost any bandpass spatial filter followed by a rectifier will suffice to expose this motion to standard analysis. The following quilt requires a more specifically tuned texture-grabbing spatial filter.

4.2.3. Stimulus: Oppositely oriented, randomly contrast-reversing squarewaves selected by a drifting grating. In Fig. 7d are displayed the four frames comprising another binary texture quilt also constructed using technique 4.2.1. Figure 7c shows the functions f_1, f_2, f_3, and f_4 used in the construction. Each of these frames was constructed by using the corresponding frame of the probabilistically defined, rightward stepping sinusoid of Fig. 7a to sample between the two squarewave gratings shown in Figs. 7b1 and 7b2. The texture quilt realized in Fig. 7d is derived by randomly reversing the contrast of each of the frames of Fig. 7c. For the realization given in Fig. 7d, the random variables ϕ_1, ϕ_2, ϕ_3 and ϕ_4 used to multiply the frames of Fig. 7c take the values -1, -1, 1, and 1 respectively.

Sinusoidal texture quilts.

It is simple to elaborate technique 4.2.1 to a method for constructing quilts involving textures of arbitrarily many contrast values. We illustrate the principle in the construction of a generic quilt comprised of patches of sinusoidal grating and we provide two specific examples.

4.2.4. A general technique for constructing sinusoidal texture quilts microbalanced under all purely temporal transformations. A generic sinusoidal quilt has N frames. Pixels of each frame are filled by choosing between a pair of sinusoids assigned to that frame. The critical constraints (to insure that the resulting stimulus will be microbalanced under all purely temporal transformations) are that the different sinusoids thus patched together, within a given frame and across different frames, must be of equal amplitude and have jointly independent, uniformly distributed random phases.

Specifically, for $i = 1, 2, ..., N$, with N the number of frames comprising the quilt, let W_i be a function, temporally constant within frame i, assigning either 1 or -1 to all points (x, y, t) in the i^{th} frame, and 0 to all points outside the i^{th} frame. We use W_i to sample between static sinusoidal gratings with random phases and different spatial frequencies. Apparent motion can often be generated with such displays by shifting each successive sampling function W_{i+1} in a fixed direction relative to W_i.

Let

$$\omega_1, \theta_1, \tilde{\omega}_1, \tilde{\theta}_1, \omega_2, \theta_2, \tilde{\omega}_2, \tilde{\theta}_2, \ldots, \omega_N, \theta_N, \tilde{\omega}_N, \tilde{\theta}_N$$

be integers. For each frame i of the texture quilt being constructed we shall use W_i to sample between two sinusoids, C_i and $\tilde{C}_i$. For some integer P (independent of frame), C_i has a spatial frequency of ω_i/P cycles per horizontal pixel and θ_i/P cycles per vertical pixel. $\tilde{C}_i$ has a spatial frequency of $\tilde{\omega}_i/P$ cycles per horizontal pixel and $\tilde{\theta}_i/P$ cycles per vertical pixel.

The phases of all of the sinusoids patched together in the quilt are independent random variables. To be precise, let

$$\rho_1, \tilde{\rho}_1, \rho_2, \tilde{\rho}_2, \ldots, \rho_N, \tilde{\rho}_N,$$

be jointly independent random variables, each assuming with equal probability a value from amongst the integers $0, 1, ..., P-1$. Then for all $(x, y, t) \in \mathbf{Z}^3$ set

$$S = \sum_{i=1}^{N} S_i,$$

where, for each i,

$$S_i[x, y, t] = \begin{cases} cos\,(2\pi(\omega_i x + \theta_i y + \rho_i)/P) & \text{if } W_i[x, y, t] = 1, \\ cos\,(2\pi(\tilde{\omega}_i x + \tilde{\theta}_i y + \tilde{\rho}_i)/P) & \text{if } W_i[x, y, t] = -1, \\ 0 & \textit{otherwise.} \end{cases}$$

Like the generic binary texture quilt B, S is microbalanced under all purely temporal transformations [27].

4.2.5. Stimulus: Oppositely oriented, random-phased sinusoids selected by a drifting grating. The sinusoidal analog to the binary texture quilt of Fig. 7d is shown in Fig. 8b. In Fig. 8a are shown the functions W_1, W_2, W_3, and W_4 used to select between horizontal and vertical gratings. For this quilt, $\tilde{\omega}_i = \theta_i = 0$, for $i = 1, 2, 3, 4$; and for some integer F (with F/P the number of cycles per pixel), $\omega_i = \tilde{\theta}_i = F$.

The motion displayed by the texture quilt of Fig. 8b evidently depends on the difference in orientation between the textures mixed in each frame. Of course, we can just as easily keep orientation constant and vary spatial frequency instead.

4.2.6. Stimulus: Random-phased sinusoids of different spatial frequencies, selected by a drifting grating. Figure 8c shows a texture quilt using the sampling functions of Fig. 8a, but setting $\omega_i = \theta_i = 2\tilde{\omega}_i = 2\tilde{\theta}_i$ for $i = 1, 2, ..., 4$.

The empirical observations with texture quilts are that motion can be perceived when texture patches move across the field, even when the texture-conveyed motion is contrived so that there are no spatiotemporal correlations in the stimulus to support standard motion analysis [11,17], and when second-order temporal processing can be excluded [27]. These texture-conveyed motions are detected by convolving the input stimulus with a spatial texture-grabbing filter tuned to the moving texture, then rectifying the output of the filter (to indicate the presence or absence of the texture), and subjecting the rectified output to standard motion analysis. That supraordinate texture orientation is easily perceived in the x, y representations of the texture-conveyed motion (Figs. 7d, 8b and 8c) indicates that there exists second-order orientation processing of textures in the space domain analogous to the second-order motion processing of textures in the motion domain.

5. Summary.

Section 1 introduced the distinction between first- and second-order motion mechanisms. Section 2 reviewed the fundamental results concerning drift-balanced and microbalanced random stimuli. Microbalanced random stimuli are useful in the study of second-order motion perception because (i) they are guaranteed *not to systematically stimulate* first-order (Fourier-energy analytic or autocorrelational) motion mechanisms, and (ii) it is easy to produce microbalanced random stimuli that display consistent, compelling apparent motion across independent realizations.

Section 3 described microbalanced random stimuli that displayed different types of apparent motion. The contrast-modulating squarewave (Stimulus 3.1) suggests that some instances of microbalanced motion may be exposed to standard motion analysis by simple rectification. The contrast-reversing squarewave (stimulus 3.2) suggests that other instances of microbalanced motion are exposed by rectifying the temporal derivative of the stimulus. Moreover, the motion of stimulus 3.1 can *not* be exposed by temporal differentiation followed by rectification, whereas the motion of stimulus 3.2 can *not* be exposed by simple rectification. A temporal filter with the impulse response given in Fig. 5 (including terms for both temporal differentiation and temporal identity), followed by rectification, does suffice to expose the motion of both stimuli 3.1 and 3.2 to standard motion analysis. For each of these stimuli, the optimal *spatial* filter to expose the motion is the identity.

Section 4 introduced the notion of a random stimulus *microbalanced under all pointwise transformations*. Section 4.1 provided necessary and sufficient conditions for a random stimulus to be of this sort. Such stimuli I are significant because pointwise transformations applied directly to I merely result again in microbalanced random functions; thus the first

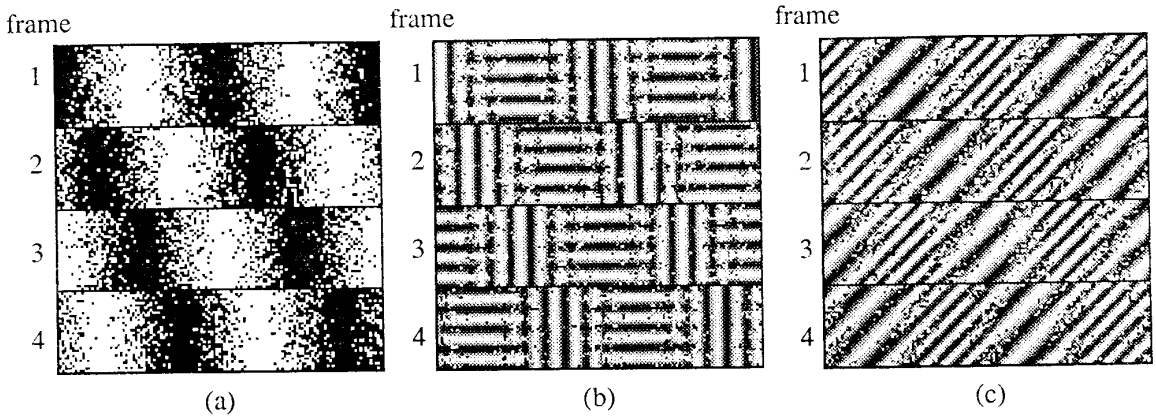

Figure 8: *Sinusoidal texture quilts—motion driven by differences in orientation or in spatial frequency.* The 4 frames in (a) are used to select between two sinusoidal patterns. Stimuli (b) and (c) are realizations of two such random stimuli, each of which is microbalanced under all purely temporal transformations. The sinusoids mixed in (b) differ in orientation, while the sinusoids mixed in (c) have the same orientation, but differ in spatial frequency. The phases of sinusoids are jointly independent across frames, and across sinusoids of different frequency mixed in the same frame.

transformation in any respect effective at exposing I's motion to analysis must be non-pointwise. If the transformations applied to the visual signal are limited to cascades of (i) linear shift-invariant operators and (ii) pointwise operators, then the first processing stage effective in revealing the motion of I must be a nontrivial linear transformation. Moreover, since I is microbalanced, this linear filter must be followed by at least a pointwise nonlinearity for I's motion to be revealed to standard analysis.

Section 4.2 illustrated random stimuli—*texture quilts* (stimuli 4.2.2, 4.2.3, 4.2.5 and 4.2.6)—that yielded compelling texture-conveyed apparent motion. These stimuli were microbalanced under all purely temporal transformations. Their motion cannot be exposed by simple rectification, nor indeed by any *purely temporal* transformations, no matter how nonlinear. The perception of texture quilt motion can be modeled in terms of a *spatial* texture-grabbing filter followed by rectification and standard motion analysis. Thus, the minimal system to account for all the demonstrations of second-order motion perception presented here would consist of a temporal filter that has both an identity and a temporal differentiation component, a band-selective spatial filter followed by a rectifier and standard motion analysis.

Acknowledgements.

The research reported here was supported by USAF Life Science Directorate, Visual Information Processing Program, Grants 85-0364 and 88-0140.

References

[1] Adelson, E.H. and J. Bergen, "Spatiotemporal energy models for the perception of motion," *J. Opt. Soc. Am. A*, **2**, 2, 284-299, 1985.

[2] Watson, A.B. and A.J. Ahumada, "A model of human visual-motion sensing," *J. Opt. Soc. Am. A*, **2**, 2, 322-342, 1985.

[3] van Santen, J.P.H. and G. Sperling, "A Temporal Covariance Model of Motion Perception," *J. Opt. Soc. Am. A*, **1**, 451-473, 1984.

[4] van Santen, J.P.H. and G. Sperling, "Elaborated Reichardt Detectors," *J. Opt. Soc. Am. A*, **2**, 2, 300-321, 1985.

[5] Heeger, D.J., "A model for the extraction of image flow," *J. Opt. Soc. Am. A*, **4**, 8, 1455-1471, 1987.

[6] Watson, A.B. and A.J. Ahumada, "A Look at Motion in the Frequency Domain," NASA Technical Memorandum 84352, 1983.

[7] Marr, D. and S. Ullman, "Directional selectivity and its use in early visual processing," *Proc. R. Soc. Lond. B.*, **211**, 151-180.

[8] Marr, D. *Vision*, W. H. Freeman & Co., 1982.

[9] Anandan, P. "A unified perspective on computational techniques for the measurement of visual motion," *DARPA IU workshop proc.*, 1987.

[10] Waxman, A. M. and F. Bergholm, "Convected activation profiles and image flow extraction," *Laboratory for Sensory Robotics Technical Report 4*, College of Engineering, Boston U., 1987.

[11] Ramachandran, V.S., V.M. Rao and T.R. Vidyasagar, "Apparent movement with subjective contours," *Vision Res.*, **13**, 1399-1401, 1973.

[12] Sperling, G., "Movement perception in computer-driven visual displays," *Behavior Research Methods and Instrumentation*, **8**, 144-151, 1976.

[13] Petersik, J.T., K.I. Hicks and A. Pantle, "Apparent movement of successively generated subjective figures," *Perception*, **7**, 371-383, 1978.

[14] Lelkins, A.M.M. & J.J. Koenderink, "Illusory motion in visual displays," *Vision Res.*, *24*, 1083-1090, 1984.

[15] Cavanagh, P., J. Boeglin and O.E. Favreau, "Perception of motion in equiluminous kinematograms," *Perception*, **14**, 151-162, 1985.

[16] Derrington, A.M. and D.R. Badcock, "Separate detectors for simple and complex grating patterns?" *Vision Res.*, **25**, 1869-1878, 1985.

[17] Green, M., "What determines correspondence strength in apparent motion," *Vision Res.*, **26**, 599-607, 1986.

[18] Prazdny, K., "What variables control (long range) apparent motion?" *Perception*, **15**, 37-40, 1986.

[19] Pantle, A. and K. Turano, "Direct comparisons of apparent motions produced with luminance, contrast-modulated (CM), and texture gratings" *Investigative Ophthalmology and Visual Science*, **27**, *3*, 1986.

[20] Derrington, A.M. and G.B. Henning, "Errors in direction-of-motion discrimination with complex stimuli," *Vision Res.*, **27**, 61-75, 1987.

[21] Turano, K. and A. Pantle, "On the mechanism that encodes the movement of contrast variations - I: velocity discrimination," submitted.

[22] Bowne, S.B., S.P. McKee, & D.A. Glaser, "Motion interference in speed discrimination," in press.

[23] Cavanagh, P., Arguin, M. and M. von Grunau, "Inter-attribute apparent motion," in press.

[24] Chubb, C. and G. Sperling, "Drift-balanced random stimuli: A general basis for studying non-Fourier motion perception," *Investigative Ophthalmology and Visual Science*, **28**, p. 233, 1987.

[25] Chubb, C. and G. Sperling, "Processing stages in non-Fourier motion perception," *Investigative Ophthalmology and Visual Science*, **28**, p. 266, 1988.

[26] Chubb, C. and G. Sperling, "Drift-balanced random stimuli: A general basis for studying non-Fourier motion perception," *J. Opt. Soc. Am. A.*, **5**, *11*, 1986-2007, 1988.

[27] Chubb, C. and G. Sperling, "Texture quilts: basic tools for studying motion from texture," *Mathematical Studies in Perception and Cognition*, 88-1, New York University, Department of Psychology, 1988.

[28] Chubb, C. and G. Sperling, "Two motion-perception mechanisms revealed through distance-driven reversal of apparent motion," *Proc. Natl. Acad. Sci. USA*, **86**, 1988, in press.

[29] Watson, A.B., A.J. Ahumada and J.E. Farrell, "The window of visibility: A psychophysical theory of fidelity in time-sampled motion displays," NASA Technical Paper 2211, 1983.

[30] Watson, A.B., A.J. Ahumada and J.E. Farrell, "The window of visibility: A psychophysical theory of fidelity in time-sampled motion displays," *J. Opt. Soc. Am. A*, **3**, *3*, 300-307, 1986.

[31] Reichardt, W., "Autocorrelation, a principle for the evaluation of sensory information by the central nervous system," in *Sensory Communication*, W. A. Rosenblith, ed., Wiley, New York, 1961.

[32] Caelli, T., "Three processing characteristics of visual texture segregation," *Spatial Vision*, **1**, *1*, 19-30, 1985.

[33] Bergen, J.R. and E.H. Adelson, "Early vision and texture perception," *Nature*, **333**, *6171*, 363-364, 1988.

[34] Sutter, A., J. Beck and N. Graham, "Contrast and spatial variables in texture segregation: testing a simple spatial frequency channels model," in press.